Controlling Third-Order Nonlinearities by Ion-Implantation Quantum-Well Intermixing

Sean J. Wagner, *Member, IEEE*, Barry M. Holmes, *Member, IEEE*, Usman Younis, Amr S. Helmy, *Senior Member, IEEE*, David C. Hutchings, *Senior Member, IEEE*, and J. Stewart Aitchison, *Senior Member, IEEE*

***Abstract*—The optical Kerr effect was measured by observing self-phase modulation in GaAs–AlGaAs superlattice-core waveguides modified by ion-implantation quantum-well intermixing. The band-gap energy was shifted by 68 nm for an implantation dose of 0.5×10^{13} cm^{-2} and annealing temperature of 775 °C. The Kerr effect was suppressed by up to 71% in the transverse-electric polarization after intermixing. A reduced polarization dependence of the self-phase modulation was observed after intermixing.**

***Index Terms*—Nonlinear optics, optical Kerr effect, quantum-well intermixing (QWI), semiconductor superlattice.**

COMPOUND semiconductors have led the way towards monolithically integrated all-optical signal processing devices. Mature fabrication technologies have allowed the development of low-loss waveguides and advanced structures such as Bragg reflection waveguides [1], passive mode converters [2], and cascaded microring resonators [3]. AlGaAs is of particular interest since the optical Kerr effect, a third-order nonlinearity, has been shown to be 500 times stronger than in silica [4]. These nonlinearities are nonresonant and do not rely on free-carrier plasma dispersion effects since the operating wavelengths are typically below the half-band-gap energy. This has opened the possibility of all-optical switching devices such as nonlinear directional couplers (NLDCs) [5] and nonlinear Mach–Zehnder interferometers (NLMZIs) [6] with ultrafast response times necessary for ultrahigh-speed communications systems and signal processing. Multiple quantum-well (MQW) structures based on AlGaAs permit greater flexibility to tailor the band-gap energy to suit the optical properties required for particular applications. Furthermore, the band-gap energy of MQWs can be modified after wafer growth by quantum-well intermixing (QWI) techniques [7]. This cost-effective approach allows selective control of the electronic and optical properties of the material in specific regions defined using standard lithographic techniques. Already, QWI has been utilized to fabricate NLMZIs [8], asymmetric nonlinear waveguides for soliton emission [9], and quasi-phase-matching (QPM) gratings [10]. While several QWI methods are available, ion-implantation-induced QWI has been shown to produce superior resolution [11], which is a requirement for devices such as QPM gratings. Deep-well semiconductor superlattices have attracted attention as the greater fill-factor and large band discontinuity in comparison to conventional quantum-well structures potentially provides a larger modification to nonresonant optical properties such as the refractive index and nonlinear optical susceptibilities in the transparency window for the complete structure. Thus, shorter and more efficient devices that require less power to operate are possible. In this letter, we demonstrate large modifications of the optical Kerr effect in GaAs–AlGaAs superlattice-core waveguides induced by ion-implantation QWI at wavelengths near the half-band-gap.

We have previously reported on the large polarization dependence of the Kerr coefficient in GaAs–AlAs superlattice waveguides [12]. However, measurements indicated the presence of parasitic two-photon absorption (TPA) resonances due to the reduced barrier resulting in asymmetric quantum wells (ASQW) found on either side of the superlattice waveguide core. In the present study, we modified the waveguide structure with several improvements. The new core layer was a 600-nm-thick superlattice of 75 periods each with 14 : 14 monolayers of GaAs : $Al_{0.85}Ga_{0.15}As$. The $Al_{0.85}Ga_{0.15}As$ layers were substituted for the AlAs layers in the original superlattice to avoid the detrimental effects of oxidation. However, this change reduced the maximum band-gap change achievable over the previous superlattice, and thus the maximum achievable modulation in the nonlinear optical coefficients. Also, the superlattice waveguide core was terminated on both sides with barrier $Al_{0.85}Ga_{0.15}As$ layers instead of GaAs to avoid the formation of reduced potential barriers with the adjacent buffer layers which consisted of 300-nm-thick $Al_{0.56}Ga_{0.44}As$. Cladding layers were 800-nm-thick $Al_{0.60}Ga_{0.40}As$. A second lower cladding layer of 1-μm-thick $Al_{0.85}Ga_{0.15}As$ was added to improve confinement of the optical mode to the core layer. All layers were grown on a semi-insulating GaAs substrate by molecular beam epitaxy.

Intermixed superlattice samples were prepared by using the ion-implantation method. As^{2+} ions were implanted with an energy of 4 MeV at a dosage of 0.5×10^{13} cm^{-2}. Rapid thermal annealing of the implanted samples was carried out for 60 s at a temperature of 775 °C. Fig. 1 shows low-temperature (77 K) photoluminescence (PL) measurements of as-grown and intermixed samples. The PL peak for the as-grown material

Manuscript received August 06, 2008; revised September 18, 2008. First published October 31, 2008; current version published January 14, 2009. This work was supported by grants from the U.K. Engineering and Physical Science Research Council, and the Natural Science and Engineering Research Council of Canada. The work of S. J. Wagner was supported by an NSERC Postgraduate Scholarship. The work of U. Younis was supported by the NUST SEECS.

S. J. Wagner, A. S. Helmy, and J. S. Aitchison are with the Edward S. Rogers Sr. Department of Electrical and Computer Engineering, University of Toronto, 10 King's College Road, Toronto, Ontario, M5S 3G4, Canada (e-mail: sean.wagner@utoronto.ca).

B. M. Holmes, U. Younis, and D. C. Hutchings are with the Department of Electronics and Electrical Engineering, University of Glasgow, Glasgow, G12 8QQ, Scotland, UK.

Color versions of one or more of the figures in this letter are available online at http://ieeexplore.ieee.org.

Digital Object Identifier 10.1109/LPT.2008.2008629

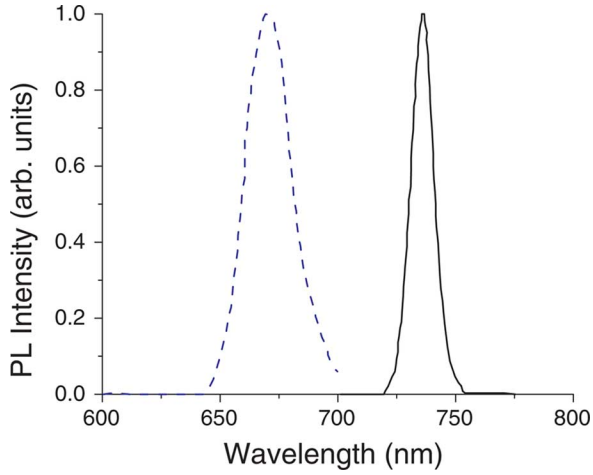

Fig. 1. PL spectra for as-grown (black solid) and intermixed (blue dashed) superlattice at 77 K.

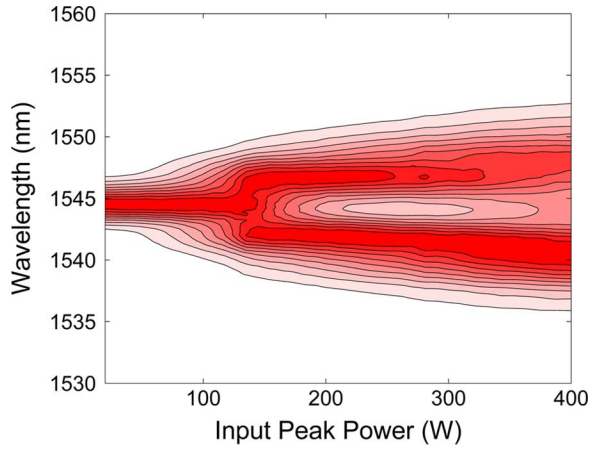

Fig. 2. Measured spectral broadening in as-grown waveguides at 1545 nm in the TM polarization.

places the half-band-gap energy within the 1550-nm telecommunications band. Intermixing shifted the PL peak by 68 nm, which is larger than the 40-nm shifts achieved with a conventional MQW [13]. Strip-loaded waveguides, each 3.0 μm wide and 1.0 μm deep were fabricated using reactive ion etching for both as-grown and intermixed samples. Linear losses were measured using the Fabry–Pérot method. For as-grown waveguides, loss coefficients averaged 0.55 cm^{-1} for wavelengths around 1550 nm, while intermixed waveguides had average losses of 0.65 cm^{-1}. Additional samples with ion doses of up to 5×10^{13} cm^{-2} were also prepared and showed PL shifts of up to 85 nm, but with increasing values for the optical loss. The 0.5×10^{13} cm^{-2} dose gave an appropriate balance between optical losses and band-gap shift.

Characterization of the waveguides was carried out using a singly-resonant optical parametric oscillator synchronously pumped by a mode-locked Ti : sapphire laser. Output pulses were 1.3–2.0 ps long at a repetition rate of 75.6 MHz. Light was end-fire coupled into waveguide samples using a $40\times$ objective lens with average powers of up to 250 mW. Spectral changes induced by self-phase modulation were recorded at the waveguide output with an optical spectrum analyzer as the input power was increased for both transverse-electric (TE) and transverse-magnetic (TM) polarized inputs. Fig. 2 shows the evolution of the output spectrum with input peak power for the TM mode in the 5.7 mm-long as-grown sample at a center wavelength of 1545 nm. The point at which the spectrum splits into two peaks with a maximum dip in the middle is identified as the point where the nonlinear phase shift is 1.5π. Ordinarily, the value of n_2 is calculated by using this point as a reference. However, this simplistic method can underestimate the n_2 by as much as 100%, especially since nonlinear absorption is not included in the calculation. It is potentially necessary to account for TPA, three-photon absorption (3PA), group-velocity dispersion (GVD), pulse shape, and chirp. The nonlinear Schrödinger equation (NLSE) describing the propagation of a pulse under such conditions can be written as

$$j\frac{\partial A}{\partial z} + j\frac{\alpha_0}{2} + j\frac{\alpha_2}{2}\frac{|A|^2}{A_{\text{eff}}^{(3)}}A + j\frac{\alpha_3}{2}\left[\frac{|A|^2}{A_{\text{eff}}^{(5)}}\right]^2 A - \frac{\beta_2}{2}\frac{\partial^2 A}{\partial t^2} + \frac{2\pi n_2}{\lambda}\frac{|A|^2}{A_{\text{eff}}^{(3)}}A = 0 \quad (1)$$

where $A(t, z)$ is the pulse envelope and represents the square root of the optical power, and α_0 is the linear loss coefficient. The TPA and 3PA coefficients, α_2 and α_3, were determined by a combination of inverse transmission methods [4] and numerical fits of the transmission curves. GVD coefficients β_2 were calculated from the dispersion of the effective index of the waveguides reported in [14]. $A_{\text{eff}}^{(3)}$ and $A_{\text{eff}}^{(5)}$ are the third- and fifth-order effective mode areas which are defined in [4] and were calculated to be between 4.5 and 6.0 μm^2 over the wavelength span of interest. Pulses were modeled as chirped super-Gaussian in shape. The NLSE was solved numerically using the split-step Fourier method [15] to obtain simulated spectral evolution plots. The simulation was repeated for various values of the waveguide effective n_2 until the calculated spectral evolution matched the measured data.

The n_2 values obtained from matching the spectral broadening were that of the waveguide structure as a whole. To evaluate the behaviour of the superlattice layer before and after intermixing, it was necessary to deconvolve the value of n_2 for the core layer alone. This was done by accounting for the overlap of the optical mode with the buffer and cladding layers [12]. The value of n_2 in those layers was calculated from measured values of bulk $Al_{0.18}Ga_{0.82}As$ [4] and the scaling laws for n_2 [16]. The resulting core layer n_2 values for as-grown and intermixed superlattice are shown in Fig. 3. Error bars reflect uncertainties in the linear loss, $A_{\text{eff}}^{(3)}$, and pulse chirp, and the variance in n_2 which gives matched spectral patterns. The magnitude of the measured values is similar to bulk $Al_{0.18}Ga_{0.82}As$ [4]. However, n_2 is smaller than in the previous superlattice structure [12], which is attributed to a elimination of parasitic ASQWs in the new superlattice structure. A strong polarization anisotropy is observed in both superlattice structures with the TE polarization having n_2 values nearly three times larger than the TM polarization in the present structure. This is due to lifting of the light-/heavy-hole valance band degeneracy which places the half-band-gap resonance of the TM polarization at a shorter wavelength than the TE polarization [17]. Intermixed superlattice had n_2 values suppressed by as much as 71% in the TE polarization and 33% in the TM polarization. The polarization dependence after intermixing was substantially reduced, which

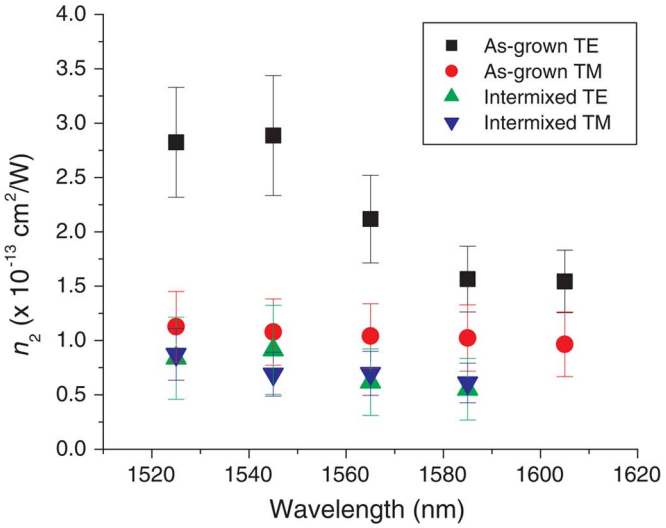

Fig. 3. Measured n_2 values for as-grown and intermixed superlattice.

indicated that the superlattice reverted to a more bulk-like material.

In comparison to previous work on intermixing MQW waveguides [13], the observed suppression of n_2 in the superlattice is up to 11% larger. Furthermore, the present intermixing technique and dosage is less traumatic to the underlying crystalline structure, i.e., it is not fully intermixed with commensurate lower optical losses, and provides a higher spatial resolution. The new superlattice improves over the previous superlattice structure with a reduction in parasitic TPA. This yields a better nonlinear figure-of-merit, defined as $T = 2\alpha_2\lambda/n_2$ [12]. For 1545 and 1565 nm in the TE mode, $T < 0.5$ which indicates that complete switching in an NLDC is possible. At 1525 nm, which is above the half-band-gap energy, TPA increased significantly and the value of T was above the required value of 1. Above 1565 nm, TPA is nonexistent and 3PA becomes the dominant nonlinear loss mechanism. However, suppression of n_2 after intermixing is significantly reduced at these longer wavelengths. Thus, optimal wavelengths for switching are between 1545 and 1565 nm which are close enough to the half-band-gap resonance to enhance n_2 while still having low TPA values.

In conclusion, suppression of the Kerr effect was measured in GaAs–AlGaAs superlattice-core waveguides after QWI by ion implantation. Ion doses of 0.5×10^{13} cm^{-2} resulted in a 68-nm shift of the PL peak after annealing. Values for n_2 were reduced in the intermixed superlattice by as much as 71% in the TE mode due to shifting of the half-band-gap resonance. An observed polarization anisotropy to n_2 of 63% in the as-grown superlattice was substantially reduced in the intermixed material.

ACKNOWLEDGMENT

The authors would like to thank the University of Surrey Ion Beam Centre for carrying out the ion implantation. They also acknowledge the efforts by the technical support staff of the James Watt Nanofabrication Centre at the University of Glasgow.

REFERENCES

[1] B. Bijlani, P. Abolghasem, and A. S. Helmy, "Second harmonic generation in ridge Bragg reflection waveguides," *Appl. Phys. Lett.*, vol. 92, no. 10, pp. 101 124–3, 2008.

[2] B. M. Holmes and D. C. Hutchings, "Realization of novel low-loss monolithically integrated passive waveguide mode converters," *IEEE Photon. Technol. Lett.*, vol. 18, no. 1, pp. 43–45, Jan. 1, 2006.

[3] R. Grover, V. Van, T. A. Ibrahim, P. P. Absil, L. C. Calhoun, F. G. Johnson, J. V. Hryniewicz, and P.-T. Ho, "Parallel-cascaded semiconductor microring resonators for high-order and wide-FSR filters," *J. Lightw. Technol.*, vol. 20, no. 5, pp. 900–905, May 2002.

[4] J. S. Aitchison, D. C. Hutchings, J. U. Kang, G. I. Stegeman, and A. Villeneuve, "The nonlinear optical properties of AlGaAs at the half band gap," *IEEE J. Quantum Electron.*, vol. 33, no. 3, pp. 341–348, Mar. 1997.

[5] J. S. Aitchison, A. H. Kean, C. N. Ironside, A. Villeneuve, and G. I. Stegeman, "Ultrafast all-optical switching in $Al_{0.18}Ga_{0.28}As$ directional coupler in 1.55 μm spectral region," *Electron. Lett.*, vol. 27, no. 19, pp. 1709–1710, 1991.

[6] K. Al-Hemyari, J. S. Aitchison, C. N. Ironside, G. T. Kennedy, R. S. Grant, and W. Sibbett, "Ultrafast all-optical switching in GaAlAs integrated interferometer in 1.55 μm spectral region," *Electron. Lett.*, vol. 28, no. 12, pp. 1090–1092, 1992.

[7] J. H. Marsh, "Quantum well intermixing," *Semi. Sci. Technol.*, vol. 6, pp. 1136–1155, 1993.

[8] A. M. Kan'an, P. Li Kam Wa, Mitra-Dutta, and J. Pamulapati, "Area-selective disordering of multiple quantum well structures and its applications to all-optical devices," *J. Appl. Phys.*, vol. 80, no. 6, pp. 3179–3183, 1996.

[9] P. Dumais, A. Villeneuve, A. Saher-Helmy, J. S. Aitchison, L. Friedrich, R. A. Fuerst, and G. I. Stegeman, "Toward soliton emission in asymmetric GaAs/AlGaAs multiple-quantum-well waveguide structures below the half-bandgap," *Opt. Lett.*, vol. 25, no. 17, pp. 1282–1284, 2000.

[10] K. Zeaiter, D. C. Hutchings, R. M. Gwilliam, K. Moutzouris, S. V. Rao, and M. Ebrahimzadeh, "Quasi-phase-matched second-harmonic generation in a GaAs/AlAs superlattice waveguide by ion-implantation-induced intermixing," *Opt. Lett.*, vol. 28, no. 11, pp. 911–913, 2003.

[11] P. Scrutton, M. Sorel, D. C. Hutchings, J. S. Aitchison, and A. S. Helmy, "Characterizing bandgap gratings in GaAs : AlAs superlattice structures using interface phonons," *IEEE Photon. Technol. Lett.*, vol. 19, no. 9, pp. 677–679, May 1, 2007.

[12] S. J. Wagner, J. Meier, A. S. Helmy, J. S. Aitchison, M. Sorel, and D. C. Hutchings, "Polarization-dependent nonlinear refraction and iwo-photon absorption in GaAs/AlAs superlattice waveguides below the half-bandgap," *J. Opt. Soc. Amer. B*, vol. 24, no. 7, pp. 1557–1563, 2007.

[13] C. J. Hamilton, J. H. Marsh, D. C. Hutchings, J. S. Aitchison, G. T. Kennedy, and W. Sibbett, "Localized Kerr-type nonlinearities in GaAs/AlGaAs multiple quantum well structures at 1.55 μm," *Appl. Phys. Lett.*, vol. 68, no. 22, pp. 3078–3080, 1996.

[14] T. C. Kleckner, A. S. Helmy, K. Zeaiter, D. C. Hutchings, and J. S. Aitchison, "Dispersion and modulation of the linear optical properties of GaAs–AlAs superlattice waveguides using quantum-well intermixing," *IEEE J. Quantum Electron.*, vol. 42, no. 3, pp. 280–286, Mar. 2006.

[15] G. P. Agrawal, *Nonlinear Fiber Optics*, 2nd ed. San Diego: Academic, 1995.

[16] M. Sheik-Bahae, D. C. Hutchings, D. J. Hagan, and E. W. Van Slryland, "Dispersion of bound electron nonlinear refraction in solids," *IEEE J. Quantum Electron.*, vol. 27, no. 6, pp. 1296–1309, Jun. 1991.

[17] D. C. Hutchings, "Theory of ultrafast nonlinear refraction in semiconductor superlattices," *IEEE J. Sel. Topics Quantum Electron.*, vol. 10, no. 5, pp. 1124–1132, Sep./Oct. 2004.